

---

This is an electronic reprint of the original article.  
This reprint may differ from the original in pagination and typographic detail.

Shevchenko, Andriy; Grahn, P.; Kaivola, M.

## Functional optical metamaterials employing spatial dispersion and absorption

*Published in:*

Proceedings of SPIE - The International Society for Optical Engineering

*DOI:*

[10.1117/12.2060808](https://doi.org/10.1117/12.2060808)

Published: 01/01/2014

*Document Version*

Publisher's PDF, also known as Version of record

*Please cite the original version:*

Shevchenko, A., Grahn, P., & Kaivola, M. (2014). Functional optical metamaterials employing spatial dispersion and absorption. *Proceedings of SPIE - The International Society for Optical Engineering*, 9160, 1-8. Article 91600S. <https://doi.org/10.1117/12.2060808>

---

This material is protected by copyright and other intellectual property rights, and duplication or sale of all or part of any of the repository collections is not permitted, except that material may be duplicated by you for your research use or educational purposes in electronic or print form. You must obtain permission for any other use. Electronic or print copies may not be offered, whether for sale or otherwise to anyone who is not an authorised user.

# PROCEEDINGS OF SPIE

[SPIDigitalLibrary.org/conference-proceedings-of-spie](https://SPIDigitalLibrary.org/conference-proceedings-of-spie)

## Functional optical metamaterials employing spatial dispersion and absorption

A. Shevchenko, P. Grahn, M. Kaivola

A. Shevchenko, P. Grahn, M. Kaivola, "Functional optical metamaterials employing spatial dispersion and absorption," Proc. SPIE 9160, Metamaterials: Fundamentals and Applications 2014, 91600S (12 September 2014); doi: 10.1117/12.2060808

**SPIE.**

Event: SPIE NanoScience + Engineering, 2014, San Diego, California, United States

# Functional optical metamaterials employing spatial dispersion and absorption

A. Shevchenko, P. Grahn, M. Kaivola

Department of Applied Physics, Aalto University, P.O. Box 13500, FI-00076 Aalto, Finland

## ABSTRACT

Functional optical metamaterials usually consist of absorbing, anisotropic and often non-centrosymmetric structures of a size that is only a few times smaller than the wavelength of visible light. If the structures would be substantially smaller, excitation of higher-order electromagnetic multipoles in them, including magnetic dipoles, would be inefficient. As a result, the material would act as an ordinary electric-dipole material. The required non-negligible size of metamolecules, however, makes the material spatially dispersive, so that its optical characteristics depend on light propagation direction. This phenomenon significantly complicates the description of metamaterials in terms of conventional electric permittivity and magnetic permeability tensors. In this work, we present a simple semianalytical method to describe such spatially dispersive metamaterials, which are also allowed to be optically anisotropic and non-centrosymmetric. Applying the method, we show that a strong spatial dispersion, combined with absorption and optical anisotropy, can be used to efficiently control propagational characteristics of optical beams.

**Keywords:** metamaterials, spatial dispersion, optical absorption, refractive index and impedance, self-collimation

## 1. INTRODUCTION

Optical metamaterials are nanostructured artificial materials with extraordinary optical properties that are obtained by designing the material's structural units. It is usually required that these units, called metamolecules, support the excitation of both electric and magnetic dipole moments, since then the refractive index ( $n$ ) and the wave impedance ( $Z$ ) of the material can independently be tuned over a wide range of values. Some of the key examples of existing and future applications of such materials are near-field focusing and imaging elements,<sup>1–5</sup> such as a "perfect lens"<sup>6</sup> (here one could choose, e.g.,  $n = -1$ ), elements enhancing optical density of states and energy transfer<sup>7,8</sup> as well as coherence<sup>9–11</sup> (e.g., if  $n = 0$ ), and aberration-free non-refractive elements<sup>12</sup> (with  $n = 1$ ). For applications like these, the material should be optically homogeneous, isotropic and spatially non-dispersive. In addition, the wave impedance and the imaginary part of the refractive index of the material should be close to those in vacuum ( $Z_0 \approx 377 \Omega$  and  $0$ , respectively). Otherwise, the reflection and absorption of light would significantly hamper the desired application. For other applications, such as optical cloaking,<sup>13,14</sup> one can in contrast need optical inhomogeneity and anisotropy, but optical absorption and spatial dispersion should still be absent. Practical realization of all these applications faces some fundamental problems. In order to be able to significantly adjust the optical response of a metamaterial, even to obtain  $n = 1$ , the metamolecules must have pronounced multipole resonances close to the wavelength of interest. This is usually achieved with plasmon resonant excitations in metal metamolecules, in which case the material is absorptive, or with Mie resonances in high-refractive-index dielectric structures.<sup>15</sup> In both cases, for the higher-order multipole resonances to be strong, the metamolecules must be relatively large, say, not more than an order of magnitude smaller than the wavelength. Otherwise the magnetic dipole and all other higher-order resonances will vanish.<sup>16</sup> This requirement, in turn, leads to an inevitable spatial dispersion<sup>17,18</sup> that is commonly considered as an unwanted effect, because it complicates and often makes impractical the description of metamaterials in terms of traditional electric permittivity and magnetic permeability tensors. Furthermore, the optical parameters can turn out to significantly depend on the number of layers in a metamaterial slab.<sup>19,20</sup> Then, however, the structure is difficult to treat as a material.<sup>21</sup> Sometimes such metamaterials are said to be not homogenizable.

---

Further author information: (Send correspondence to A. Shevchenko)

A. Shevchenko: E-mail: andriy.shevchenko@aalto.fi, Telephone: +358 50 4333956

Metamaterials: Fundamentals and Applications 2014, edited by Nader Engheta, Mikhail A. Noginov, Nikolay I. Zheludev,  
Proc. of SPIE Vol. 9160, 91600S · © 2014 SPIE · CCC code: 0277-786X/14/\$18 · doi: 10.1117/12.2060808

In this work, we describe a method for accurate and simple theoretical description of a general metamaterial that can be spatially dispersive, anisotropic, non-centrosymmetric and, in addition, internally twisted, i.e. allowing its metamolecules to be tilted with respect to the crystal lattice.<sup>23</sup> Then, instead of avoiding or reducing the effect of spatial dispersion, we search for useful applications of metamaterials, in which this effect is significant. Examples of such applications are position-independent diffraction-free guidance of optical beams and apertureless spatial filtering of beams reflected from the metamaterial's surface. For the second application, it is even preferable that the material is optically absorptive.

## 2. RETRIEVAL OF REFRACTIVE INDEX AND WAVE IMPEDANCE

If the metamaterial is spatially dispersive, the parameters  $n$  and  $Z$  can still be introduced for optical plane waves propagating in the material and having different values for different propagation directions of the waves. Therefore, they are called the effective *wave* parameters. If, in addition, the material is optically anisotropic, it is easier to use scalar  $n$  and  $Z$  for each of the two inherent polarization modes of the material (e.g., TE- and TM-polarized) than to treat the material in terms of tensorial quantities. Furthermore, if the metamolecular layers in the material are separated such that the gap between them is much smaller than the period  $\Lambda_z$  ( $\mathbf{z}$  is perpendicular to the layers), the interlayer evanescent-wave coupling can take place, as a result of which the effective wave parameters will depend on the number of layers in the slab. The retrieval of the effective wave parameters, using the Fresnel transmission and reflection coefficients  $\tau_F$  and  $\rho_F$  at each boundary, is still possible for such slabs. In some cases, the parameter values can converge when the number of molecular layers is increased.<sup>19,20</sup> However, we have previously shown that if the metamolecules are not centrosymmetric, two counterpropagating waves can exhibit different impedances.<sup>18,22</sup> Also, if the metamaterial is internally twisted, then, at an oblique angle of incidence, the incident and reflected waves inside the material can experience different refractive indices. In these cases, the Fresnel coefficients must be modified. For a boundary separating two non-centrosymmetric internally twisted metamaterials, at  $z = 0$ , the coefficients can be written as<sup>23</sup>

$$\tau_F = \frac{\gamma_{z,i}/(\gamma_i Z_i^\sigma) + \gamma_{z,r}/(\gamma_r Z_r^\sigma)}{\gamma_{z,r}/(\gamma_r Z_r^\sigma) + \gamma_{z,t}/(\gamma_t Z_t^\sigma)} \left( \frac{Z_i}{Z_t} \right)^{(\sigma-1)/2}, \quad (1)$$

$$\rho_F = \frac{\gamma_{z,i}/(\gamma_i Z_i^\sigma) - \gamma_{z,t}/(\gamma_t Z_t^\sigma)}{\gamma_{z,r}/(\gamma_r Z_r^\sigma) + \gamma_{z,t}/(\gamma_t Z_t^\sigma)} \left( -\frac{Z_i}{Z_r} \right)^{(\sigma-1)/2}. \quad (2)$$

Here, the incident plane wave has a wave vector  $(\gamma_x, \gamma_y, \gamma_{z,i})$ , wave number  $\gamma_i = n_i k_0$  and wave impedance  $Z_i$  ( $k_0$  is the wave number in vacuum). The corresponding characteristics of the wave reflected by the interface are  $(\gamma_x, \gamma_y, -\gamma_{z,r})$  and  $Z_r$ . For ordinary materials, one would obtain  $\gamma_{z,r} = \gamma_{z,i}$ ,  $\gamma_r = \gamma_i$  and  $Z_r = Z_i$ . The wave transmitted by the interface is characterized by  $(\gamma_x, \gamma_y, \gamma_{z,t})$ ,  $\gamma_t = n_t k_0$  and  $Z_t$ . The parameter  $\sigma$  is equal to  $\pm 1$  for the TE and TM polarization, respectively. When dealing with asymmetric metamaterials, such as those composed of classical split-ring resonators, one must use Eqs. (1) and (2) for evaluation of  $n$  and  $Z$  instead of applying traditional Fresnel coefficients.

If the interlayer separation is such that the evanescent-wave coupling between the layers is negligible, the wave parameters are independent of the number of layers and, therefore, one can obtain  $n$  and  $Z$  from a single metamolecular layer.<sup>18,23</sup> This substantially simplifies the computational problem to be solved. The retrieval procedure in this case is as follows. Since usually the metamolecules are imbedded in a certain dielectric host medium, we denote the wave vector in this medium by  $\mathbf{k}$  and the wave number by  $k$ . Then, a single layer of metamolecules in an infinite host medium is considered. At a given incidence angle  $\theta$ , the layer transmission and reflection coefficients  $\tau_1, \tau_2, \rho_1$  and  $\rho_2$  are calculated numerically with respect to the central plane of the layer. Here,  $\tau_1$  and  $\rho_1$  are obtained when the wave is incident from one side of the layer (at angle  $\theta$ ) and  $\tau_2$  and  $\rho_2$  are calculated for illumination from the opposite direction (at angle  $180^\circ - \theta$ ). Note that, if the metamolecules are centrosymmetric and possess reflection symmetry with respect to the layer, calculation of  $\tau_2$  and  $\rho_2$  is not needed, since  $\tau_1 = \tau_2$  and  $\rho_1 = \rho_2$ .

In the next step, the phase-shifted coefficients  $f_1 = \tau_1 \exp(ik_z \Lambda_z)$ ,  $f_2 = \tau_2 \exp(ik_z \Lambda_z)$ ,  $g_1 = \rho_1 \exp(ik_z \Lambda_z)$  and  $g_2 = \rho_2 \exp(ik_z \Lambda_z)$  are obtained and substituted into the expressions

$$\alpha = f_2 + f_1^{-1}(1 - g_1 g_2), \quad (3)$$

$$\beta = f_2 / f_1. \quad (4)$$

The effective refractive index is then calculated from

$$n^2 k_0^2 = k_x^2 + k_y^2 + \gamma_z^2, \quad (5)$$

where

$$\gamma_z = -\frac{i}{\Lambda_z} \ln \left[ \frac{\alpha}{2\beta} \pm \left( \frac{\alpha^2}{4\beta^2} - \frac{1}{\beta} \right)^{1/2} \right] + \frac{2\pi m}{\Lambda_z}. \quad (6)$$

In Eq. (6),  $m$  is an integer number that must satisfy the requirement that  $\gamma_z$  and  $n$  have positive imaginary parts and continuous spectra with physically justified (e.g., Maxwell-Garnett) values at long wavelengths. The effective wave impedance is calculated from

$$Z = Z_h \left( \frac{k\gamma_z}{k_z\gamma} \right)^p \frac{g_2 + [1 - f_1 \exp(-i\gamma_z\Lambda_z)]}{g_2 - [1 - f_1 \exp(-i\gamma_z\Lambda_z)]}, \quad (7)$$

where  $Z_h$  is the impedance of the host medium and  $p$  is equal to  $+1$  and  $-1$  for TE- and TM-polarized waves, respectively. The retrieved scalar effective wave parameters  $n$  and  $Z$  along with their dependence on the wave frequency, propagation direction and polarization form a complete macroscopic description of a metamaterial that is allowed to be spatially dispersive, anisotropic, non-centrosymmetric and internally twisted. The approach has been proven to yield very good agreement with direct numerical calculations.<sup>23</sup>

### 3. DESCRIPTION OF OPTICAL BEAMS

In order to be able to describe propagation of optical beams through spatially dispersive metamaterials, we use the fact that any beam can be treated as a linear superposition of monochromatic plane waves. This plane-wave decomposition is called angular-spectrum representation.<sup>24</sup> For a single-frequency continuous-wave beam that propagates in positive  $z$ -direction, the electric field distribution at a fixed  $z$  can be written as

$$\mathbf{E}(x, y; z) = \int_{-\infty}^{\infty} \int_{-\infty}^{\infty} \hat{\mathbf{E}}(k_x, k_y; z) e^{i[k_x x + k_y y]} dk_x dk_y, \quad (8)$$

where each plane-wave complex amplitude  $\hat{\mathbf{E}}(k_x, k_y; z)$  is connected to its value at  $z = 0$  by  $\hat{\mathbf{E}}(k_x, k_y; z) = \hat{\mathbf{E}}(k_x, k_y; 0) e^{ik_z z}$ . Equation (8) represents an inverse Fourier transform. The amplitudes  $\hat{\mathbf{E}}(k_x, k_y; z)$  are given by the direct Fourier transform

$$\hat{\mathbf{E}}(k_x, k_y; z) = \frac{1}{4\pi^2} \int_{-\infty}^{\infty} \int_{-\infty}^{\infty} \mathbf{E}(x, y; z) e^{-i[k_x x + k_y y]} dk_x dk_y. \quad (9)$$

When treating the interaction of optical beams with metamaterial slabs, the following procedure can be used. The incident beam, for which the electric-field distribution  $\mathbf{E}(x, y; z)$  is known, is decomposed into plane waves with complex amplitudes  $\hat{\mathbf{E}}(k_x, k_y; z)$ , which are found from Eq. (9). At the boundary (assumed to be located at  $z = 0$ ), each of these plane waves is split into the reflected and transmitted waves, the amplitudes of which at  $z = 0$  are found from  $\hat{E}_r(k_x, k_y; 0) = \rho_F \hat{E}(k_x, k_y; 0)$  and  $\hat{E}_t(k_x, k_y; 0) = \tau_F \hat{E}(k_x, k_y; 0)$ , respectively. Note that  $\rho_F$  and  $\tau_F$  are also functions of  $k_x$  and  $k_y$ . Then, using Eq. (8), we obtain the distributions

$$\mathbf{E}_r(x, y; z) = \int_{-\infty}^{\infty} \int_{-\infty}^{\infty} \hat{\mathbf{E}}_r(k_x, k_y; 0) e^{i[k_x x + k_y y - k_z z]} dk_x dk_y \quad (10)$$

for the reflected beam (propagating in the negative  $z$ -direction) and

$$\mathbf{E}_t(x, y; z) = \int_{-\infty}^{\infty} \int_{-\infty}^{\infty} \hat{\mathbf{E}}_t(k_x, k_y; 0) e^{i[k_x x + k_y y + \gamma_z z]} dk_x dk_y \quad (11)$$

for the beam transmitted by the boundary into the metamaterial [ $\gamma_z$  is given by Eq. (6)]. It should be noted that even if the beam is linearly polarized (e.g., in the plane of incidence), both TE and TM-polarized plane-wave components will *in general* be present in the expansion. On the other hand, if the beam is not focused tightly,

this feature can be ignored. Without going into detail of this decomposition, we see immediately that, if within the limits of the angular spread of the beam,  $\gamma_z$  is by design independent of  $k_x$  and  $k_y$ , then the factor  $e^{i\gamma_z z}$  can be removed from the integral in Eq. (11). In this special case, the distribution  $\mathbf{E}_t(x, y; z)$  will obey the relation

$$\mathbf{E}_t(x, y; z) = \mathbf{E}_t(x, y; 0)e^{i\gamma_z z}. \quad (12)$$

This result shows that except for a possible attenuation of the beam in the  $z$ -direction (since  $\gamma_z$  is complex), its transverse intensity profile stays the same across the metamaterial slab. The beam is therefore guided to the other side of the slab without divergence, and the angle of refraction *for the beam* is equal to 0. This effect is similar to the self-collimation effect observed in photonic crystals.<sup>25–27</sup> If the metamaterial is internally twisted, the beam can be refracted in an arbitrary direction (not only along the normal), because some other component of the wave vector can be designed to be constant within the range of the beam’s angular spectrum. Furthermore, analyzing Eq. (10), one can see that if  $\rho_F$  depends on  $k_x$  and  $k_y$ , the angular spectrum of the *reflected* field will differ from that of the incident field. This suggests applications in apertureless spatial filtering.

#### 4. EXAMPLES

As an example, we consider a metamaterial that is optically anisotropic, non-centrosymmetric and internally twisted. It consists of metamolecules in the form of asymmetric paired silver discs and has a lattice constant of 120 nm. The metamolecules are tilted with respect to the lattice by an angle of  $\alpha = 45^\circ$ ;  $\alpha$  is shown in Fig. 1(a). We have chosen these dimer metamolecules, since they exhibit significant magnetic dipole and electric quadrupole polarizabilities<sup>28</sup> and strong spatial dispersion<sup>29</sup> in the visible spectral range. We have previously

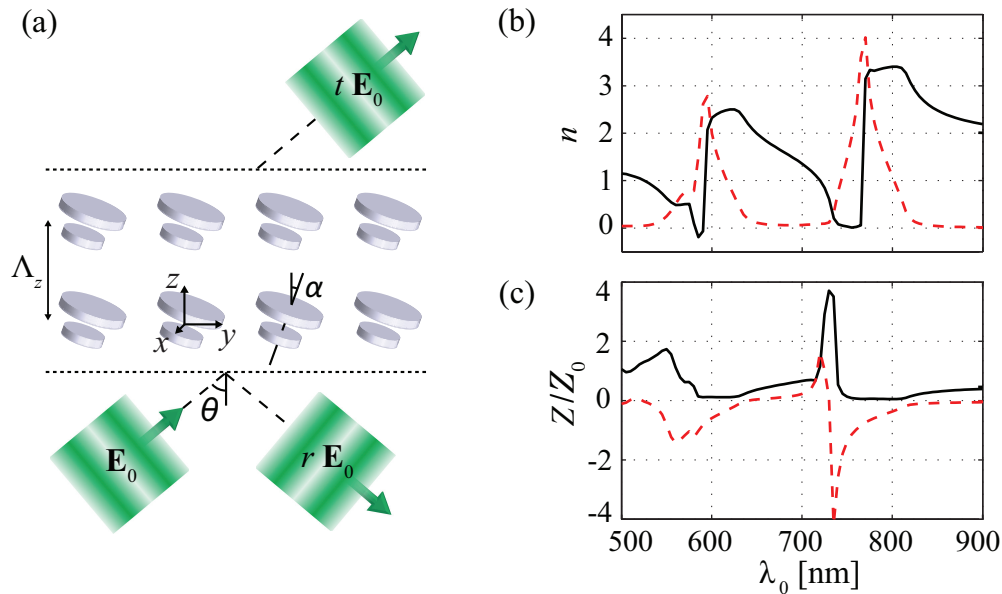


Figure 1. A dimer metamaterial (a) and the effective refractive index (b) and wave impedance (c) evaluated for a TE-polarized plane wave with  $\theta = \alpha = 45^\circ$ . The real and imaginary parts are shown by solid and dashed lines, respectively.  $Z_0$  is the impedance of vacuum.

shown that the dominant higher-order multipole excitation in such particles is composed of linear currents in the two discs, which oscillate out-of-phase with respect to each other.<sup>30</sup> The radii of the larger and smaller discs are chosen to be 40 nm and 25 nm, respectively. The discs have a thickness of 10 nm and they are separated by a surface-to-surface distance of 20 nm. The coordinate system used in the calculations is chosen to have the  $z$ -axis directed along the normal to the metamaterial surface, and the metamolecules are tilted in the  $yz$ -plane with respect to this axis [see Fig. 1(a)]. The angle of incidence of a plane wave is denoted by  $\theta$ , and the plane of incidence coincides with the  $yz$ -plane. Also, when  $\theta$  is equal to  $\alpha$ , the wave is incident from the smaller-disc side.

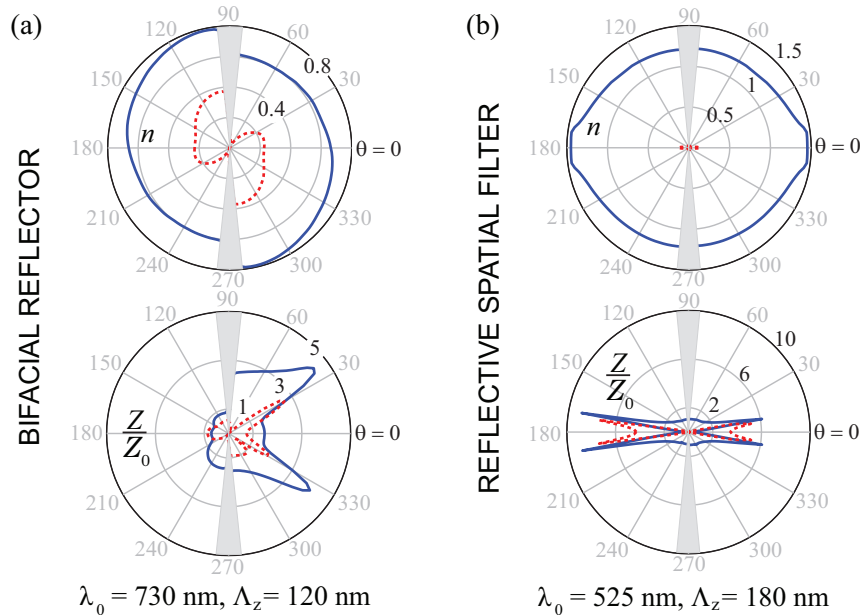


Figure 2. The dependence of the wave parameters on the incidence angle  $\theta$  for a dimer metamaterial acting as (a) a bifacial reflector and (b) a reflective spatial filter. The materials differ by the parameters  $\lambda_0$  and  $\Lambda_z$ , which are  $\lambda_0 = 730$  nm and  $\Lambda_z = 120$  nm in (a) and  $\lambda_0 = 525$  nm and  $\Lambda_z = 180$  nm in (b). The waves are assumed to be TE-polarized. The real and imaginary parts of the quantities are shown by solid and dashed lines, respectively. The gray sectors mark the range of angles excluded from the calculations.

The dielectric host medium is assumed to have a refractive index of 1.5. The effective wave parameters  $n$  and  $Z$  of the metamaterial are calculated by applying the retrieval procedure presented in section 2. The numerical calculations were performed using the computer software COMSOL Multiphysics and the values for the refractive index of silver were taken from Ref. 31. Figures 1(b) and (c) show the spectra of the wave parameters retrieved for a TE-polarized wave incident at an angle  $\theta = \alpha = 45^\circ$ . In the refractive index spectrum, one can distinguish the electric-dipole resonances of the two discs composing the dimer. It can be seen that at certain wavelengths, the real part of the refractive index takes values close to zero and even becomes negative.

Figure 2(a) shows the refractive index and impedance evaluated for this material considering TE-polarized waves at a fixed wavelength of 730 nm with incidence angles from 0 to  $360^\circ$ . The material is considered to be surrounded by glass. The incidence angles close to  $\pm 90^\circ$  are excluded from the calculations (see the grey sectors). The refractive index has rather low values of the real part and relatively high values of the imaginary part [see the solid and dashed curves, respectively, in the top polar plot of Fig. 2(a)]. The imaginary part, however, substantially decreases when the incidence angle exceeds  $45^\circ$ . The values of the refractive index are seen to be equal for two opposite illumination directions [ $n(\theta) = n(\theta + 180^\circ)$ ], which fulfils optical reciprocity. The impedance, however, is far from being centrosymmetric. For example, at  $\theta \approx 220^\circ$  the medium is nearly impedance-matched to vacuum, while at  $\theta \approx 40^\circ$  the impedance is four times larger than that in vacuum. This means that a layer of the material will efficiently reflect light by its front surface, e.g., at  $\theta = 40^\circ$ , but show a low reflection, when the wave is incident from the opposite direction, at  $\theta = 220^\circ$ . The layer will therefore act as a *bifacial reflector*.

Next, in order to enhance the sensitivity of the wave reflection coefficient to the incidence angle, we increase the crystal's period in the  $z$ -direction only, to 180 nm, and set the wavelength to 525 nm. This brings the material close to the Bragg reflection regime for incidence angles around  $\theta = 0$ . Figure 2(b) shows the refractive index and impedance evaluated as functions of the incidence angle for plane waves incident on the material from glass. The polar plot of the real part of  $n$  is flat near  $\theta = 0$ , revealing a photonic-crystal-type self-collimation effect. At these incidence angles, however, the imaginary part of the wave impedance is high, implying that the

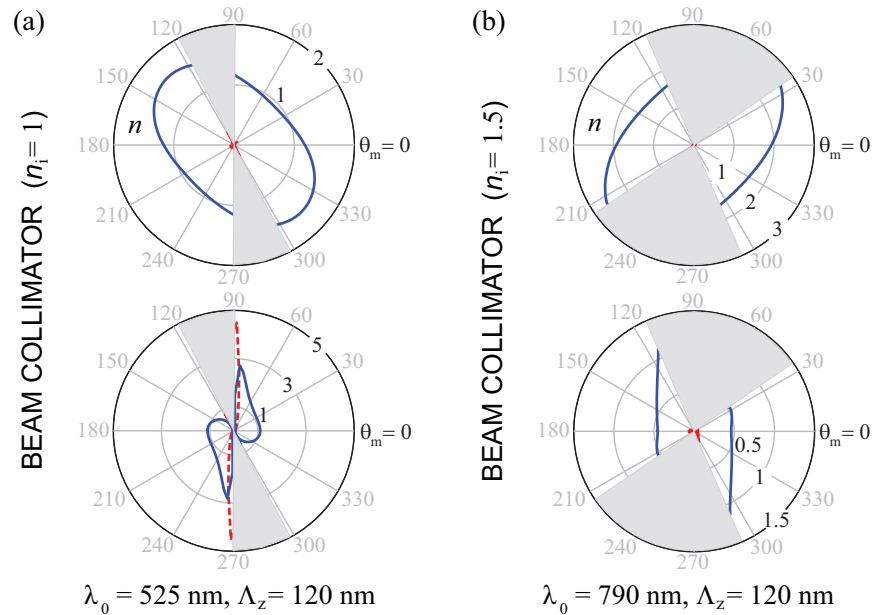


Figure 3. The dependence of the wave parameters on the wave propagation angle  $\theta_m$  in the considered dimer metamaterial with  $\Lambda_z = 120$  nm. The waves are TM-polarized. The metamaterial can be used as a low-loss self-collimating waveguide (a) in vacuum at  $\lambda_0 = 525$  nm and (b) in glass at  $\lambda_0 = 790$  nm. In (a), the beam propagation angle in the material is about  $45^\circ$  (or  $225^\circ$ ), and in (b), this angle is equal to  $-45^\circ$  (or  $135^\circ$ ). The real and imaginary parts of the quantities are shown by solid and dashed lines, respectively. The gray sectors show the range of angles that were not considered in the calculations.

waves will be reflected from the surface of the material rather than transmitted into the material. On the other hand, at  $\theta > 30^\circ$ , the impedance approaches the value  $Z_0$  in vacuum, which means that the reflection coefficient approaches 0. Thus, an optical beam with a divergence angle of, say,  $\beta = 60^\circ$  will upon the reflection at normal incidence be converted into a beam with  $\beta \approx 10^\circ$ . The material will therefore act as a *reflective spatial filter* that is independent of the location of the focal spot. Since the strong angular dependence of  $n$  and  $Z$  is in this example determined by  $\Lambda_z$  rather than the shape and orientation of the dimers, similar filtering will take place also in the orthogonal direction (for plane waves with  $\mathbf{k}$  in the  $xz$ -plane).

For a slab of a metamaterial to be used as a self-collimating waveguide, the material should have (i) a flat contour of the real part of  $n$  as a function of the propagation angle  $\theta_m$  in the medium, (ii) a small imaginary part of  $n$  and (iii) an impedance close to that of the surrounding medium. Here we consider 2D self-collimation (in the  $yz$ -plane) similar to that in 2D photonic crystals.<sup>25–27</sup> For the considered metamaterial with  $\Lambda_z = 120$  nm, these conditions are well satisfied at the wavelengths of 525 nm [see Fig. 3(a)] and 790 nm [Fig. 3(b)] for TM-polarized waves. In Fig. 3, the gray sectors show the range of angles that we do not consider in the calculations. At 525 nm, the real part of  $n$  has quite a flat contour and the impedance is close to  $Z_0$  in the range of  $\theta_m$  from 0 to about  $60^\circ$ . A slab of this material can therefore be used as a *beam self-collimator* for light coupled into the slab from *vacuum* at an incidence angle of  $\theta \approx 30^\circ$ . Inside the material, the beam will propagate at an angle of about  $45^\circ$  with substantially reduced divergence. In the second case (at  $\lambda_0 = 790$  nm), the real part of  $n$  is also nearly flat for  $\theta_m$  between  $-65^\circ$  and about  $-25^\circ$ . Within this range, the values of  $n$  and  $Z$  are close to those in glass and the imaginary part of  $n$  is even smaller than in the previous case. Therefore, the material can be used as a *self-collimator* for a beam incident from *glass* at an angle close to  $-45^\circ$ . The beam will propagate in the material with reduced divergence exactly at an angle of  $-45^\circ$ . We note that metamaterials, with a lattice constant  $\Lambda$  smaller than half a wavelength  $\lambda_h/2$  in the host medium, have not been previously demonstrated to exhibit the self-collimation effect. Compared with self-collimating photonic crystals that operate close to the Bragg reflection regime with  $\Lambda > \lambda_h/2$ , metamaterials can be designed to be impedance-matched to the surrounding medium, which will improve coupling of light into the artificial waveguide.

## 5. CONCLUSIONS

We have presented a recipe for evaluating the optical wave parameters  $n$  and  $Z$  for a general spatially dispersive, anisotropic, non-centrosymmetric and internally twisted metamaterial. If the material exhibits significant interlayer evanescent-wave coupling, the retrieval procedure can be quite time consuming for thick metamaterial layers and the retrieved wave parameters can depend on the number of layers in the slab. If, on the other hand, this coupling is weak or absent, the parameters can be obtained very fast for an arbitrarily thick slab by considering numerically only a single layer of metamolecules.

The fact that, the complex plane-wave parameters  $n$  and  $Z$  depend on the wave propagation direction in spatially dispersive metamaterials can be used to modify the angular spectrum and to control propagational characteristics of optical beams. Applying the model to a particular metamaterial, composed of tilted metal dimers, we have calculated  $n$  and  $Z$  in a broad spectral range for various propagation directions and different polarizations of the waves and shown that spatially dispersive and absorptive metamaterial slabs can be used as bifacial reflectors, position-independent apertureless spatial filters and low-loss self-collimating waveguides. These examples demonstrate high potential of such metamaterials for creation of flat optical elements with demanding functional abilities.

## REFERENCES

1. Parimi, P. V., Lu, W. T., Vodo, P. and Sridhar, S., "Photonic crystals: Imaging by flat lens using negative refraction," *Nature* **426**, 404 (2003), <http://dx.doi.org/10.1038/426404a>.
2. Fang, N., Lee, H., Sun, C. and Zhang, X., "Subdiffraction-limited optical imaging with a silver superlens," *Science* **308**, 534-537 (2005), <http://dx.doi.org/10.1126/science.1108759>.
3. Liu, Z., Lee, H., Xiong, Y., Sun, C. and Zhang, X., "Far-field optical hyperlens magnifying sub-diffraction-limited objects," *Science* **315**, 1686 (2007), <http://dx.doi.org/10.1126/science.1137368>.
4. Kawata, S., Inouye, Y. and Verma, P., "Plasmonics for near-field nano-imaging and superlensing," *Nature Photonics* **3**, 388-394 (2009), <http://dx.doi.org/10.1038/nphoton.2009.111>.
5. Casse, B. D. F., Lu, W. T., Huang, Y. J., Gultepe, E., Menon, L. and Sridhar, S., "Super-resolution imaging using a three-dimensional metamaterials nanolens," *Appl. Phys. Lett.* **96**, 023114 (2010), <http://dx.doi.org/10.1063/1.3291677>.
6. Pendry, J. B., "Negative refraction makes a perfect lens," *Phys. Rev. Lett.* **85**, 3966-3969 (2000), <http://dx.doi.org/10.1103/PhysRevLett.85.3966>.
7. Vesseur, E. J. R., Coenen, T., Caglayan, H., Engheta, N. and Polman, A., "Experimental verification of  $n = 0$  structures for visible light," *Phys. Rev. Lett.* **110**, 013902 (2013), <http://dx.doi.org/10.1103/PhysRevLett.110.013902>.
8. Silveirinha, M. and Engheta, N., "Tunneling of electromagnetic energy through subwavelength channels and bends using  $\epsilon$ -near-zero materials," *Phys. Rev. Lett.* **97**, 157403 (2006), <http://dx.doi.org/10.1103/PhysRevLett.97.157403>.
9. Engheta, N., "Pursuing near-zero response," *Science* **340**, 286 (2013), <http://dx.doi.org/10.1126/science.1235589>.
10. Yang, J. J., Francescato, Y., Maier, S. A., Mao, F. and Huang, M., "Mu and epsilon near zero metamaterials for perfect coherence and new antenna designs," *Opt. Express* **22** 9107-9114 (2014), <http://dx.doi.org/10.1364/OE.22.009107>.
11. Moitra, P., Yang, Y., Anderson, Z., Kravchenko, I. I., Briggs, D. P. and Valentine, J., "Realization of an all-dielectric zero-index optical metamaterial," *Nature Photonics* **7**, 791 (2013), <http://dx.doi.org/10.1038/NPHOTON.2013.214>.
12. Tuniz, A., Kuhlmeier, B. T., Chen, P. Y. and Fleming, S. C., "Weaving the invisible thread: design of an optically invisible metamaterial fibre," *Opt. Express* **18**, 18095 (2010), <http://dx.doi.org/10.1364/OE.18.018095>.
13. Pendry, J. B., Schurig, D. and Smith, D. R., "Controlling electromagnetic fields," *Science* **312**, 1780 (2006), <http://dx.doi.org/10.1126/science.1125907>.
14. Cai, W., Chettiar, U. K., Kildishev, A. V. and Shalaev, V. M., "Optical cloaking with metamaterials," *Nature Photonics* **1**, 224-227 (2007), <http://dx.doi.org/10.1038/nphoton.2007.28>.

15. Soukoulis, C. M. and Wegener, M., "Past achievements and future challenges in the development of three-dimensional photonic metamaterials," *Nature Photonics* **5**, 523-530 (2011), <http://dx.doi.org/10.1038/nphoton.2011.154>.
16. Zhou, J., Koschny, Th., Kafesaki, M., Economou, E. N., Pendry, J. B. and Soukoulis, C. M., "Saturation of the magnetic response of split-ring resonators at optical frequencies," *Phys. Rev. Lett.* **95**, 223902 (2005), <http://dx.doi.org/10.1103/PhysRevLett.95.223902>.
17. Gompf, B., Krausz, B., Frank, B. and Dressel, M., "k-dependent optics of nanostructures: Spatial dispersion of metallic nanorings and split-ring resonators," *Phys. Rev. B* **86**, 075462 (2012), <http://dx.doi.org/10.1103/PhysRevB.86.075462>.
18. Grahn, P., Shevchenko, A. and Kaivola, M., "Theoretical description of bifacial optical nanomaterials," *Opt. Express* **21**, 23471-23485 (2013), <http://dx.doi.org/10.1364/OE.21.023471>.
19. Andryieuski, A., Menzel, Ch., Rockstuhl, C., Malureanu, R., Lederer, F. and Lavrinenko, A., "Homogenization of resonant chiral metamaterials," *Phys. Rev. B* **82**, 235107 (2010), <http://dx.doi.org/10.1103/PhysRevB.82.235107>.
20. Chen, W.-C., Totachawattana, A., Fan, K., Ponsetto, J. L., Strikwerda, A. C., Zhang, X., Averitt, R. D. and Padilla, W. J., "Single-layer terahertz metamaterials with bulk optical constants," *Phys. Rev. B* **85**, 035112 (2012), <http://dx.doi.org/10.1103/PhysRevB.85.035112>.
21. Simovski, C. R., "Bloch material parameters of magneto-dielectric metamaterials and the concept of Bloch lattices," *Metamaterials* **1**, 6280 (2007), <http://dx.doi.org/10.1016/j.metmat.2007.09.002>.
22. Grahn, P., Shevchenko, A. and Kaivola, M., "Interferometric description of optical metamaterials," *New J. Phys.* **15**(11), 113044 (2013), <http://dx.doi.org/10.1088/1367-2630/15/11/113044>.
23. Grahn, P., Shevchenko, A. and Kaivola, M., "Internally twisted non-centrosymmetric optical metamaterials," *Proc. SPIE* **9125**, 91251L (2014), <http://dx.doi.org/10.1117/12.2051779>
24. Novotny, L. and Hecht, B., [*Principles of nano-optics*], Cambridge University Press, Cambridge (2006).
25. Arlandis, J., Centeno, E., Pollès, R., Moreau, A., Campos, J., Gauthier-Lafaye, O. and Monmayrant, A., "Mesoscopic self-collimation and slow light in all-positive index layered photonic crystals," *Phys. Rev. Lett.* **108**, 037401 (2012), <http://dx.doi.org/10.1103/PhysRevLett.108.037401>.
26. Lu, Z., Shi, S., Murakowski, J. A., Schneider, G. J., Schuetz, C. A. and Prather, D. W., "Experimental demonstration of self-collimation inside a three-dimensional photonic crystal," *Phys. Rev. Lett.* **96**, 173902 (2006), <http://dx.doi.org/10.1103/PhysRevLett.96.173902>.
27. Rakich, P. T., Dahlem, M. S., Tandon, S., Ibanescu, M., Soljacic, M., Petrich, G., Joannopoulos, J. D., Kolodziejski, L. A. and Ippen, E. P., "Achieving centimetre-scale supercollimation in a large-area two-dimensional photonic crystal," *Nature Mater.* **5**, 93-96 (2006), <http://dx.doi.org/10.1038/nmat1568>.
28. Grahn, P., Shevchenko, A. and Kaivola, M., "Electric dipole-free interaction of visible light with pairs of subwavelength-size silver particles," *Phys. Rev. B* **86**, 035419 (2012), <http://dx.doi.org/10.1103/PhysRevB.86.035419>.
29. Grahn, P., Shevchenko, A. and Kaivola, M., "Multipole polarizability of a nanodimer in optical waves," *J. Europ. Opt. Soc. Rap. Public.* **8**, 13009 (2013), <http://dx.doi.org/10.2971/jeos.2013.13009>.
30. Grahn, P., Shevchenko, A. and Kaivola, M., "Electromagnetic multipole theory for optical nanomaterials," *New J. Phys.* **14**(9), 093033 (2012), <http://dx.doi.org/10.1088/1367-2630/14/9/093033>.
31. Johnson, P. B. and Christy, R. W., "Optical constants of the noble metals," *Phys. Rev. B* **6**, 4370-4379 (1972), <http://dx.doi.org/10.1103/PhysRevB.6.4370>.